THEORETICA CHIMICA ACTA

Theoret. Chim. Acta (Berl.) 45, 269–281 (1977)

Theoretical Study of the Electronic Structure of Diazomethane

II. Determination of the Least-Energy Dissociation Path to CH_2 and N_2 Products

Jacques Lievin and Georges Verhaegen

Laboratoire de Chimie Physique Moléculaire, Université Libre de Bruxelles, Faculté des Sciences, 50, avenue F. D. Roosevelt, B-1050 Bruxelles, Belgium

The least-energy dissociation path of the ground state of CH_2N_2 was determined from *ab initio* calculations using in a complementary way basis sets of minimal size (STO-3G) and double-zeta (DZ) quality. The results indicate that the least-energy point of attack of the N_2 molecule on CH_2 ($^1A_1$) is roughly perpendicular to the molecular plane (93°), the C and N atoms being almost co-linear (angle C–N–N: 203° with outermost N atom pointing away from CH_2). The potential barrier of ~ 1.2 eV found previously on the C_{2v} dissociation path, disappears completely along the least-energy dissociation path (point group C_S (out-of-plane)). These findings corroborate the Woodward-Hoffman rules for this process since the outermost orbitals of the two intersecting states found in point group C_{2v} ($\ldots 2b_1$ and $\ldots 8a_1$) both correlate to the same irreducible representation ($10a'$) in point group C_S (out-of-plane).

Larger basis set calculations (DZ + polarization functions on all centers, $3d_C$ and $3d_N$ developed here), were also carried out on CH_2N_2 ($^1A_1$, $^3A_2$ and $^1A_2$) at the $^1A_1$ equilibrium geometry and on CH_2 ($^3B_1$) and N_2 ($^1\Sigma_g^+$) at their respective equilibrium geometries. These calculations, together with consideration of correlation energy differences, yield D_0^0 (CH_2N_2, $^1A_1$) = 19 kcal/mole and vertical excitation energies of 67 and 73 kcal/mole for the $^3A_2$ and $^1A_2$ states respectively. The latter value is in good agreement with the measured experimental value: 72.4 kcal/mole corresponding to the maximum of intensity in the $^1A_2 \leftarrow {}^1A_1$ absorption band.

Key words: Diazomethane, electronic structure of ~

1. Introduction

In a previous paper, hereafter referred to as I [1], we had investigated the dissociation process:

$$CH_2N_2 \rightarrow CH_2 + N_2$$

in point group C_{2v} symmetry. As had been pointed out, this *least-motion*[1] process is symmetry-forbidden [2], and accordingly a large potential barrier (~ 1.2 eV) has been found [1]. In this work, we present an investigation of the *least-energy* dissociation pathway of the ground $^1A_1$ state of CH_2N_2. The corresponding energies of the triplet states $^3A_2(^3A'')$ and $^3B_1(^3A')$ will also be reported.

In Fig. 1, we give a description of the axis convention and of the geometrical parameters to be varied.

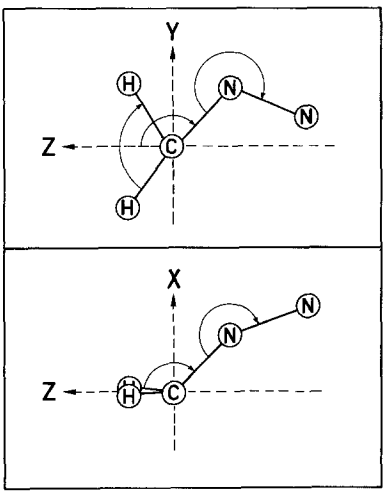

Fig. 1. Coordinate system and geometrical parameters. Throughout the text: $\theta_{HCH} = \theta$, $\theta_{H_2\text{-}C\text{-}N_2}$ (in-plane) $= \alpha_i$, $\theta_{CH_2\text{-}N\text{-}N}$ (in-plane) $= \beta_i$, $\theta_{H_2\text{-}C\text{-}N_2}$ (out-of-plane) $= \alpha_0$, and $\theta_{CH_2\text{-}N\text{-}N}$ (out-of-plane) $= \beta_0$

The states and configurations considered in I were:

$^1A_1$: (1–6) $a_1^2\ 1b_2^2\ 1b_1^2\ 7a_1^2\ 2b_2^2\ 2b_1^2$

$^1A_1^*$: (1–6) $a_1^2\ 1b_2^2\ 1b_1^2\ 7a_1^2\ 2b_2^2\ 8a_1^2$

$^3B_1$, $^1B_1$: (1–6) $a_1^2\ 1b_2^2\ 1b_1^2\ 7a_1^2\ 2b_2^2\ 2b_1 8a_1$;

in addition we shall also consider here:

$^3A_2$, $^1A_2$: (1–6) $a_1^2\ 1b_2^2\ 1b_1^2\ 7a_1^2\ 2b_2^2\ 2b_1\ 3b_2$.

Table 1 gives the necessary correlations in going from group C_{2v} to groups C_S and C_1.

Table 1. Correlations between different symmetry point-groups

C_{2v}	C_S (in-plane)	C_S (out-of-plane)	C_1
A_1	A'	A'	A
A_2	A''	A''	A
B_1	A''	A'	A
B_2	A'	A''	A

[1] With respect to symmetry group only since R_{NN} and θ_{HCH} had been optimized at all R_{CN} distances considered.

2. Methods of Calculation

Most of the results to be presented were obtained using the same programs and basis sets [3] as those described in I (mostly the double-zeta (DZ) set labelled VII [1]). Exploratory calculations were also carried out with an STO-3G minimal basis set [4] using the program GAUSSIAN 70 [5] in its closed-shell form (RHF) and in its open-shell form (UHF); the program was also modified to perform restricted open-shell calculations (OCBSE) [6]. In addition, larger calculations were carried out on the CH_2N_2, $^1A_1$, $^3A_2$, $^1A_2$ states at the equilibrium geometry of the $^1A_1$ state, and on N_2 ($^1\Sigma_g^+$) and CH_2 ($^3B_1$) at their respective equilibrium geometries using a DZ polarization-functions basis-set to be described below. Correlation energies were calculated as in I.

3. Results and Discussion

3.1. Influence of Basis Set on Geometry and Energy Variations

In group C_{2v}, the variation of four parameters had to be investigated (θ, R_{CH}, R_{CN} and R_{NN}) amongst which only one (R_{CH}) was found [1] to have a negligible influence on the reaction path. If one discards the C_{2v} geometry restriction for the least-energy dissociation path, four additional parameters have to be varied: α_i, β_i, α_0, β_0 (see Fig. 1) which makes a total of seven independent parameters.

Obviously a DZ basis set is too time-consuming for tackling this problem. That is why we chose to investigate the variation of these parameters with an STO-3G basis set. However, since it has been shown in I that the calculated equilibrium geometry and energy differences were different using an STO-3G [7] or a DZ basis-set, it was necessary to check rather carefully this dependence both on geometries and on energies.

We first checked the STO-3G basis-set dependence on the C_{2v} diabatic dissociation paths of the $^1A_1$ and $^1A_1^*$ states; the geometry and energy results are shown in Fig. 2.

As far as geometries are concerned, the results show that the θ dependency is very well rendered by the small basis-set, whereas the R_{NN} values are high. This is in keeping with the equilibrium geometries described previously at the STO-3G [7] and at the DZ [1] levels of accuracy. What is maybe more interesting is to note that for both states the R_{NN} discrepancy is virtually constant and roughly equal to 0.07 a.u. ($\sim$0.4 Å).

Energetically, the STO-3G basis-set, while describing correctly the repulsive $^1A_1^*$ state, overestimates considerably ($\sim$1.15 eV) the stability of the ground $^1A_1$ state. This effect may be rationalized in terms of basis-set borrowing. The main relative energy difference between the results using the two basis-sets is due to CH_2 ($^1A_1^*$, $1a_1^2$ $2a_1^2$ $1b_2^2$ $1b_1^2$) which is poorly described by the minimal STO-3G basis-set. More particularly one may trace the disagreement to the $1b_1$ MO which in the STO-3G calculation is composed of only one $(2p_x)_C$ basis orbital and which therefore has no

flexibility at all (LCAO coefficient = 1.0). Oppositely, the other configurations do not present the same rigidity: the CH_2N_2 $^1A_1$ configuration has two b_1 MO's and thus allows a variational optimization of the $(2p_x)_C$ and $(2p_x)_N$ coefficients; the CH_2N_2 $^1A_1^*$ and CH_2 $^1A_1$ configurations have an a_1 outermost orbital ($8a_1$ for CH_2N_2 and $3a_1$ for CH_2) which also permits a certain flexibility among the a_1 LCAO coefficients.

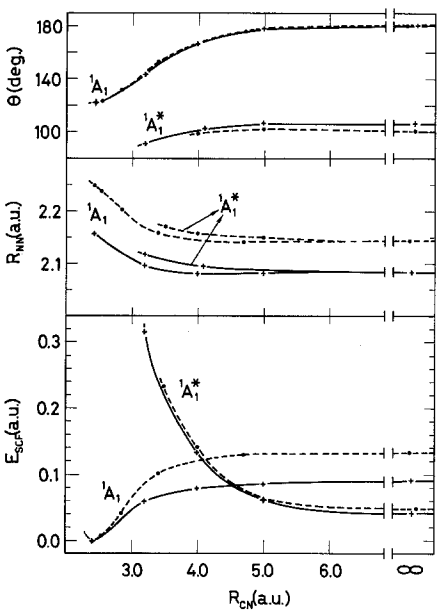

Fig. 2. Basis-set comparison: dotted lines and full circles refer to STO-3G results, full lines and crosses to DZ results. The results refer to the C_{2v} diabatic dissociation paths of the $^1A_1$ and $^1A_1^*$ states. The bottom part of the figure (E_{SCF} *vs* R_{CN}) is not a cross-section in the potential hypersurface, but a least-energy pathway (in point-group C_{2v}) corresponding to the values of the geometrical parameters given in the upper parts of the figure. The STO-3G and DZ energies are standardized at their respective equilibrium geometry for the $^1A_1$ state (E_{SCF} (STO-3G) = −145.9206 a.u.; E_{SCF} (DZ) = −147.7704 a.u.). The STO-3G results for the $^1A_1$ state come from Ref. [8]

Along the same lines, it is interesting to note that for the $^3B_1$ $(\ldots 2b_1\ 8a_1)$ and $^3A_2$ $(\ldots 2b_1\ 3b_2)$ states, to be described below, an opposite situation holds, i.e. the STO-3G energies are relatively lower ($\sim$0.02 a.u.) than that of the $^1A_1$ reference level. In this case, one may invoke the added flexibility resulting from open-shell structures which bring into play an extra symmetry orbital.

3.2. Least-Energy Dissociation Path of the $^1A_1$ State

3.2.1. Results in Point Groups C_S (in-plane) and C_1

The first "non-C_{2v}" parameter to be varied in this work is α_i. This variation is particularly interesting because it does not alter essentially the dissociation symmetry interdiction of Woodward-Hoffmann [2] since the dissociation process in point group C_S (in-plane) requires, as in point group C_{2v}, a change of symmetry of the outermost orbital (cf. Table 1).

This was borne out by a few exploratory calculations (DZ basis set) in which the angle α_i was varied from 180° (C_{2v}) to 110° at a few R_{CN} values. The results of these calculations[2] indicate clearly that the energy maximum found [1] on the C_{2v} potential energy surface does not disappear, in complete concordance with the Woodward-Hoffmann rules. More quantitatively a higher (~ 0.01 a.u.) barrier is found at smaller values of R_{CN} (~ 3.4 a.u. instead of 3.8 a.u. at $\theta = 121.7°$). This may be explained by the fact that, in CH_2, the diffuse lone-pair $(2p_z)_C$ situated behind the CH bonds reaches out the farthest for $\alpha_i = 180°$ (group C_{2v}). It follows that for smaller angles, the incoming N_2 molecule interacts with the lone-pair at smaller R_{CN} values. Additionally, a certain amount of repulsion expected with the nearest CH bound, contributes to the enhanced barrier height. It is not expected that variation of β_i would modify significantly these conclusions, although no specific tests were carried out to check this point.

Other tests were carried out with the STO-3G basis set in group C_1 to ascertain that in-plane bending does not contribute to the least-energy dissociation pathway. The results in Fig. 3 give, for different values of α (at $R_{CN} = 3.8$ a.u., $\theta = 103°$, $R_{NN} = 2.15$

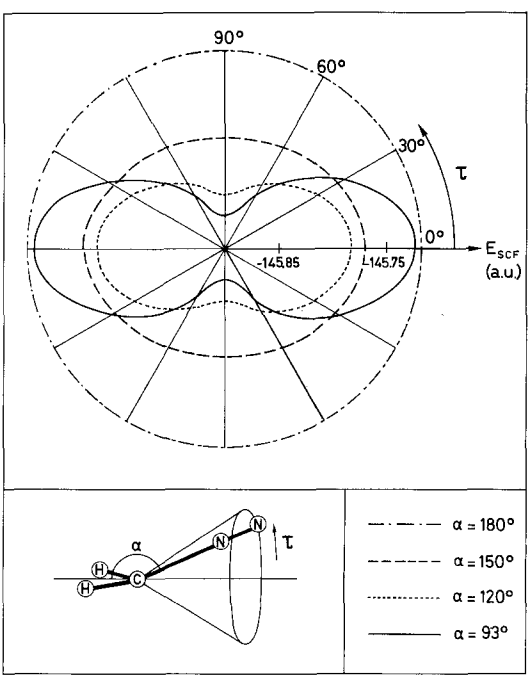

Fig. 3. Polar representation of the energy as a function of a rotational angle τ for different values of α. The energy is represented by the radial coordinate, τ by the angular coordinate. Basis set = STO-3G, $R_{CN} = 3.8$ a.u., $R_{NN} = 2.15$ a.u., $R_{CH} = 2.0385$ a.u., $\theta = 103°$, $\beta = 180°$, $\tau = 0$ for $\alpha = \alpha_i$ ($\alpha_0 = 0°$)

[2] The details of these, and other calculations, are available upon request.

a.u.) the variation of energy as a function of an angle τ which describes a cone corresponding to the rotation of a plane about the θ bisector and which contains the C–N–N axis; this rotation angle is well suited to visualize how the energy varies in going from groups C_S(in-plane) $\rightarrow C_1 \rightarrow C_S$(out-of-plane) for a given angle α (given aperture of the cone). The outermost circumference on the figure is the corresponding C_{2v} energy. The other curves show that the minimal energy is obtained for $\alpha = 93° = \alpha_0$ ($\tau = 90°$).

The energy dependence of the angle β was also investigated for in- and out-of-plane bending. This dependence was calculated for values of the other parameters corresponding to the lowest energy shown in Fig. 3: i.e. $\alpha = 93° = \alpha_0$. In a first step, the optimal value of β_0 was determined to be 203°; in a second step, the N–N axis was rotated by an angle τ' about the C–N axis keeping $\beta = 203°$. The results presented in Fig. 4 show that the C_S(out-of-plane) *trans* structure is the most stable.

These results together with those described above and in I, prove sufficiently that the determination of the dissociation path can be restricted to variation of the parameters θ, R_{NN}, α_0 and β_0 only.

Fig.4

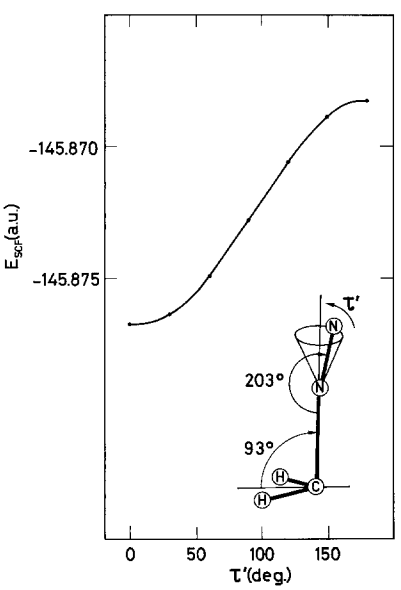

Fig.5

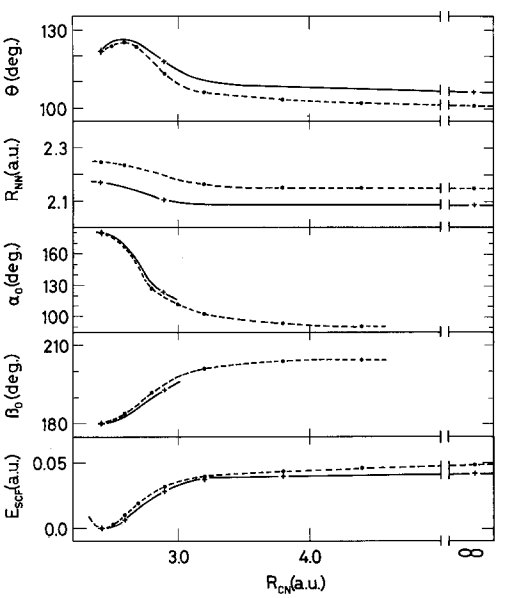

Fig. 4. Energy as a function of the rotational angle τ'. Basis set = STO-3G, $R_{CN} = 3.8$ a.u., $R_{NN} = 2.15$ a.u., $R_{CH} = 2.0385$ a.u., $\theta = 103°$, $\alpha_i = 0°$, $\alpha_0 = 93°$, $\beta = 213°$, $\tau' = 0°$ for $\beta = \beta_0$ ($\beta_1 = 0°$)

Fig. 5. Determination of dissociation path of CH_2N_2 ($^1A'$). Full circles and dashed lines indicate STO-3G calculations, crosses and full lines DZ calculations. The SCF energies have been normalized at the equilibrium geometry of the $^1A_1$ state

3.2.2. Dissociation Path (C_S out-of-plane)

The dissociation path was determined with the STO-3G basis set, and a few points along this path were checked with the larger DZ basis set. The results of these computations are shown in Fig. 5 which also gives the corresponding potential energy curves (R_{CN} *vs.* E^{SCF}) along the dissociation path.

The first point we note is that the potential barrier has disappeared completely. This is in keeping with the Woodward-Hoffmann rules since in point-group C_S (out-of-plane) the dissociation process is no longer symmetry-forbidden (cf. Table 1), and hence energetically more favourable [2].

We also note the good agreement between the STO-3G and the DZ optimization of the parameters as a function of R_{CN}, with the exception of R_{NN} for which, here again, there is a discrepancy of ~ 0.07 a.u. These findings corroborate completely the C_{2v} results presented in Sect. 3.1.

The R_{NN} variation along the dissociation path is very similar to what was found in point-group C_{2v} [1]; oppositely θ was found to vary considerably less than before[3], although there is still a small incipient increase of θ at small R_{CN} distances (~ 2.5 a.u.).

The values of the angles α_0 and β_0 along the dissociation path show that the minimal energy approach of N_2 towards CH_2 ($^1A_1$) is:

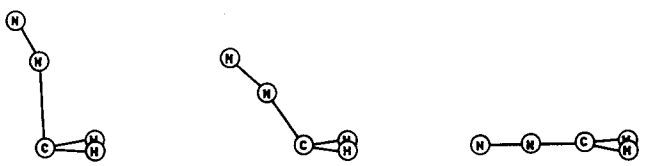

Fig. 6 shows the variation of the force constants relative to α_0 ($f(\alpha_0)$) and β_0 ($f(\beta_0)$) as a function of R_{CN}. We first note that, surprisingly, for values close to R_{CN}(eq.) $\simeq 2.4$ a.u., $f(\beta_0) > f(\alpha_0)$. This may be explained by the existence of the π structure along the C–N–N axis, above and below the CH_2 plane[4]: whereas variation of α_0 enhances the repulsion between the π bond and the CH bond densities, variation of β_0 tends to destroy the π structure altogether, whence a higher force constant for the latter angle.

As R_{CN} increases, the π structure weakens and finally results in a localized $2p_x$ lone-pair on carbon on the one hand, and a π_{u_x} MO on the N_2 molecule on the other hand. The $2p_x$ lone-pair, because of the repulsion of the two CH bond densities, shifts to

---

[3] In group C_{2v}, θ increases from $\sim 120°$ to $\sim 170°$ at $R_{CN} = 4.35$ a.u. and then abruptly decreases to $\sim 100°$ [1].

[4] At equilibrium geometry, the b_1 ($\perp$ to molecular plane) atomic populations are: 0.652 $2p_x$ (C), 0.613 $2p_x$ (N_1) and 0.735 $2p_x$ (N_2) [1].

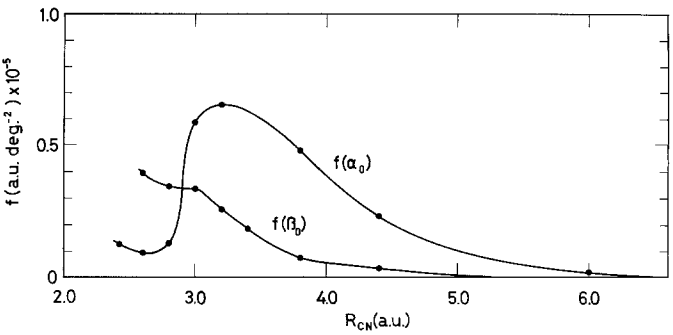

Fig. 6. Variation of force constants relative to angles α_0 and β_0 as a function of R_{CN} along the dissociation path of the $^1A'$ state

$2p_z(2p_x, 2p_z \in a'$ in point group C_S (out-of-plane)), and simultaneously α_0 decreases from 180° to 90°. The spectacular and parallel increase in $f(\alpha_0)$ may be attributed to the strong interactions resulting from the fact that the N_2 molecule with its π structure is "sandwiched" between the C–H and $2p_z$ lone-pair bond densities. In support of this interpretation we show in Fig. 7, the change in atomic population of the outermost $9a'$ orbital which describes almost exclusively the carbon lone-pair. One can see that the $2p_x \rightarrow 2p_z$ exchange and the increase in $f(\alpha_0)$ occur at the same values of R_{CN}.

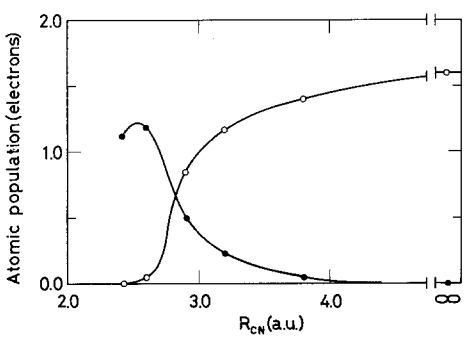

Fig. 7. Atomic populations of $2p_x$ (C) (full circles) and $2p_z$ (C) (open circles) atomic orbitals in the $9a'$ molecular orbital along $^1A'$ state dissociation path. DZ basis set

We also note that both $f(\alpha_0)$ and $f(\beta_0)$ tend to zero as R_{CN} increases reflecting the decrease in interaction between CH_2 and N_2.

Finally in Table 2, we give the energies of the $^1A_1$ ($^1A'$) state along its dissociation path, together with the energies of the $^3A_2$ ($^3A''$) and $^3B_1$ ($^3A'$) states at the corresponding geometries.

3.3. Atomic Populations

The overall gross populations [9] along the C_S (out-of-plane) dissociation path are essentially the same as those along the C_{2v} path [1]. The only major modification is in the outermost $9a'$ MO, which in the lower symmetry group C_S, allows for the

Table 2. Energies along the $^1A'$ ($^1A_1$) state dissociation path (a.u., deg.)[a]

R_{CN}	R_{NN}	θ	α_0	β_0	$E(^1A')$	$E(^3A'')$	$E(^3A')$
2.435	2.17	123	180	180	−147.7704	−147.7088	—
2.6	2.15	127	166	183	−147.7630	−147.7085	—
2.9	2.10	118	119	196	−147.7411	−147.6741	—
3.2	2.09	110	106	199	−147.7317	−147.6350	—
3.8	2.085	108	93	203	−147.7309	−147.5736	−147.706[b]
∞	2.08	106	—	—	−147.7296	—	−147.7544

[a] DZ basis set. Point group C_S (out-of-plane).
[b] See legend to Fig. 8.

change in population between the orbitals $(2p_x)_C$ and $(2p_z)_C$ at the SCF level (cf. Table 1), rather than at the CI level as in the higher symmetry group C_{2v}, as had been shown in I.

Fig. 7 shows that the population inversion along the dissociation path occurs at $R_{CN} \simeq 2.8$ a.u. This value is much smaller than what had been found in point group C_{2v} for which the "crossing-point" occurs at $R_{CN} \simeq 4.3$ a.u. The reason for this difference is that the *diabatic* dissociation pathway of the $^1A_1$ state is close to C_{2v} symmetry throughout whereas for the $^1A_1^*$ state this is not the case since for this state the incoming N_2 molecule first meets the CH_2 ($^1A_1$) lone-pair in this group (see I). As a consequence, in group C_S (out-of-plane), the "$^1A_1^*$" state becomes less repulsive, and hence crosses the "$^1A_1$" state at smaller R_{CN} values. This feature also explains the disappearance of the potential barrier.

3.4. Excited States

In addition to the dissociation path of the ground $^1A_1$ state, the $^3B_1$, $^3A_2$ and $^1A_2$ states were also considered. The two triplet states were calculated with a large basis set at the equilibrium geometry of $^1A_1$ state.

3.4.1. Triplet State Energies Along the $^1A_1$ Dissociation Path

Most of the results were obtained from the STO-3G basis set. A few points were calculated using the larger DZ basis set. Fig. 8 shows a plot of the state energies *vs.* R_{CN} (at different values of other parameters, see Table 2) and also shows the C_{2v} dissociation path of the repulsive $^3B_1$ state [1].

The most interesting feature of this figure is the crossing point of the $^1A'$ and $^3A'$ states at $R_{CN} \simeq 4.2$ a.u. This enables us to gain some insight as to the least-energy intersystem dissociation path of diazomethane: the singlet state proceeds along its diabatic dissociation path up to $R_{CN} \sim 4.2$ a.u.; follows the intersystem crossing to the $^3A'$ state[5] which decays rapidly back to the $^3B_1$ state since the C_{2v} conformation is most stable for this state at all R_{CN} distances (see Fig. 8).

[5] Halevy *et al.* [10] calculate from INDO wave-functions that the spin-orbit interaction is 34.4 cm^{-1} at the singlet-triplet crossing point.

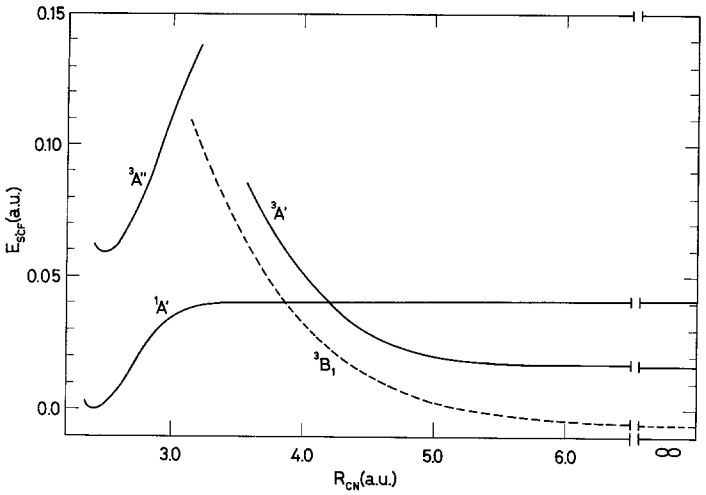

Fig. 8. SCF energies (DZ basis set) of $^1A'$, $^3A''$ and $^3A'$ states (full lines) along the $^1A'$ dissociation path (point group C_S (out-of-plane)). For comparative purposes the SCF energies (DZ basis set) of the $^3B_1$ state along its own dissociation path (point group C_{2v}) are also given (dashed line). The $^3A'$ energies were obtained indirectly because of the incompatibility of its configuration (2 open shells of same symmetry $-\cdots 9a'\ 10a'$) with the SCF program used (Whitten): the energy at $R_{CN}=\infty$ was computed directly, energies at $R_{CN}=3.6, 3.8, 4.0, 4.4$ a.u. were obtained from UHF (Ref. [5]) and OCBSE (Ref. [6]) energies (STO-3G basis-set) together with the corresponding energy differences calculated at similar geometries in point group C_{2v}

3.4.2. Vertical Excitation Energies of the $^3A_2$ and $^1A_2$ States and Dissociation Energy

In order to achieve the maximum precision in the calculation of these quantities, most calculations were performed with a more elaborate basis set for the $^1A_1$, $^3A_2$ and $^1A_2$ states of CH_2N_2 at the equilibrium geometry of the $^1A_1$ state for CH_2 ($^3B_1$) and N_2 ($^1\Sigma_g^+$) at their respective equilibrium internuclear distances.

The basis set used in these calculations is the DZ set (basis set VII in I) augmented by two-lobe $3d$ polarization functions on each heavy center (C, N_1 and N_2) and one-lobe $2p$ functions on hydrogen. The $3d$ polarization functions were taken to be identical to $3d$ correlation functions in the atoms [11], these were obtained from two-configurational numerical Hartree Fock calculations [12]. For carbon the configurations were:

$$C_1(1s^2 2s^2 2p^2) + C_2(1s^2 2s^2 3d^2) \quad (^1D \text{ state});$$

for nitrogen:

$$C_1'(1s^2 2s^2 2p^3) + C_2'(1s^2 2s^2 2p 3d^2) \quad (^2D \text{ state}).$$

The numerical $3d$ orbitals were fitted by least-square techniques [11] to two Gaussian lobes each. The parameters of these lobes are:

carbon [11]: exponents = 1.5135 and 0.3279
coefficients = 1.0 and 4.0334
lobe-separations = 0.0473 and 0.0789

nitrogen: exponents = 2.7034 and 0.5495
coefficients = 1.0 and 5.2546
lobe-separations = 0.0386 and 0.0658

The hydrogen $2p$ polarization function is that developed by Whitten [3].

The angular dependence of these polarization functions were chosen to be yz, xz and x^2-y^2 for $3d$ and y and z for $2p$.

The energies obtained with this extended basis set are summarized in Table 3 which also gives the corresponding correlation energies and the relevant vertical excitation and dissociation energies.

Table 3. Vertical excitation energies and dissociation energy

Molecule (State)	E^{a}_{SCF}(a.u.)	E^{d}_{CORR}(a.u.)	D^{0}_{0}, *V.E.* (eV)
CH_2N_2 ($^1A_1$)	−147.826[b]	−0.781[b]	0.83[e]
CH_2N_2 ($^3A_2$)	−147.754[c]	−0.746[c]	2.91[f]
CH_2N_2 ($^1A_2$)	−147.743[c]	−0.748[c]	3.16[f]
N_2($^1\Sigma_g^+$)	−108.930[b]	−0.501[b]	—
CH_2($^3B_1$)	−38.915[b]	−0.221[b]	—

[a] DZ basis set augmented by $3d$ polarization functions on C and N and $2p$ on H (see text).
[b] Calculated at DZ equilibrium geometry.
[c] Calculated at same geometry as CH_2N_2 ($^1A_1$).
[d] Obtained from minimal basis set calculation (see Ref. [1]).
[e] D^{0}_{0}, zero-point energies as in I.
[f] Vertical excitation energies (*V.E.*); differences in zero-point energies not taken into account.

The SCF results for CH_2N_2 ($^1A_1$), CH_2 and N_2 are slightly better ($\sim$0.005 a.u.) than those obtained in I; this improvement being due to a better choice of $3d$ polarization basis functions. As a result, the calculated dissociation energy is lowered by 0.08 eV ($\sim$2 kcal/mole) with respect to our former value [1].

The calculated vertical excitation energies found here for the $^3A_2$ and $^1A_2$ states are in satisfactory agreement with the values 2.65 and 2.93 eV obtained by Walch and Goddard III [12] from extended GVB-CI calculations. The $^1A_2 \leftarrow {}^1A_1$ transition has been observed experimentally and the observed band presents a maximum at 3.14 eV [14], in close agreement with our calculated value: 3.16 eV. This agreement, while being largely fortuitous because we did not take into consideration the vibrational structure of either state, nevertheless lends confidence in our calculated energies.

4. Conclusions

In this work (Parts I and II) we have investigated, quite systematically, the dissociation behaviour of the ground state and some excited states of the diazomethane molecule. To achieve this we have used in a complementary way different basis sets:

a) a minimal basis set (STO-3G) for exploratory geometry optimizations,
b) a DZ basis set for the determination of the least-energy dissociation path,
c) a DZ + polarization functions basis-set for the calculation of the dissociation energy and excitation energies.

The results of these computations show quite clearly the usefulness of the STO-3G basis set for preliminary geometry optimizations: except for R_{NN} for which a systematic error was found (constant over the whole of the potential surface), the variation of all the other parameters was found to be well represented by this minimal basis-set. This reliability allowed us to determine the least-energy dissociation path with relatively few DZ basis-set calculations.

The present work indicates that, whereas the calculated DZ equilibrium geometries seem quite precise (see I), the energies on the other hand suffer more from the lack of polarization functions in the basis-set. For example, the "DZ" energy differences (D_0^0 and *V.E.* in Table 3) differ by 0.3–0.4 eV from the corresponding DZ + polarization results. These findings are in complete agreement with a more systematic study of basis-set effects carried out recently on the valence states of CH_2 [11].

Finally, one of the interests of the present work, in our opinion, has been to illustrate, on a simple example, the orbital symmetry conservation rules as put forth by Woodward and Hoffmann [2]. We have shown in I that the C_{2v} dissociation path (symmetry-allowed by the Wigner Witmer rules) which involves a change of symmetry of the outermost orbital has a saddle-point; we have shown here that the least-energy dissociation path, for which no potential maximum subsists, proceeds in the point group of highest possible order for which the above-mentioned orbital change does not occur; this group is C_S (out-of-plane). A similar study has been carried out recently by Bauschlicher *et al.* [15] on the system CH_2 ($^1A_1$) + H_2.

Acknowledgments. The authors are grateful to Dr. M. Sana for communicating unpublished results and to Mr. D. Gervy for obtaining the 3*d*(N) polarization functions.

They acknowledge support from the Brussels University Computing Center. One of us (G.V.) is grateful to the organization FRFC (Belgium) and to the NATO Science Committee for research grants.

References

1. Lievin, J., Verhaegen, G.: Theoret. Chim. Acta (Berl.) **42**, 47 (1976)
2. Woodward, R. B., Hoffmann, R.: The conservation of orbital symmetry. Weinheim: Verlag Chemie 1970
3. Whitten, J. L.: J. Chem. Phys. **39**, 349 (1963); **44**, 359 (1966); **56**, 5458 (1972)

4. Hehre, W. J., Stewart, R. F., Pople, J. A.: J. Chem. Phys. **51**, 2657 (1969)
5. Hehre, W. J., Latham, W. A., Dichfield, R., Newton, M. D., Pople, J. A.: GAUSSIAN 70: *Ab initio* SCF-MO calculations on organic molecules. QCPE n° 236
6. Program written by Morokuma, K. Method developed by Hunt, W. J., Dunning Jr, T. H., Goddard III, W. A., Chem. Phys. Letters, **3**, 606 (1969)
7. Leroy, G., Sana, M.: Theoret. Chim. Acta (Berl.) **33**, 329 (1974)
8. Sana, M.: private communication
9. Mulliken, R. S.: J. Chem. Phys. **23**, 1833 (1955)
10. Halevi, E. A., Pauncz, R., Schek, I., Weinstein, H.: Chemical and biochemical reactivity. The Jerusalem Symposia on Quantum Chemistry and Biochemistry, VI, Israel Academy of Sciences and Humanities, Jerusalem 1974
11. Gervy, D., Verhaegen, G.: Intern. J. Quantum. Chem. (in press)
12. Froese-Fischer, C.: Comput. Phys. Commun. **1**, 151 (1969)
13. Walch, S. P., Goddard III, W. A.: J. Am. Chem. Soc. **97**, 5319 (1975)
14. Rabalais, J. W., McDonald, J. M., Scherr, V., McGlynn, S. P.: Chem. Rev. **71**, 73 (1971)
15. Bauschlicher Jr, C. W., Schaefer III, H. F., Bender, C. F.: J. Am. Chem. Soc. **98**, 1653 (1976)

Received January 27, 1977/April 1, 1977